International Journal of Bridge Engineering (IJBE), Vol.10, No.1, (2022), pp. 15-42

FORM-FINDING OF DECK-ARCH BRIDGE THROUGH GRAPHICAL AND NUMERICAL COMPUTATIONAL TOOLS

Mayank Singh

RVCA College of Architecture, Bengaluru, India
e-mail: mayanksingh.rvca@rvei.edu.in

ABSTRACT: The study deals with obtaining a design process for 2-hinged and 3-hinged deck-arches using principles of 2D graphic statics, parametric and mathematical modelling. The iterative process starts with the dead load of a straight horizontal deck and the vehicular live loads; it proceeds to incorporate the self-weight of the funicular arch and the spandrel piers. At every step the shape is modified based on funicular form finding which alters the lengths and weights of the spandrel piers which in turn affect the arch profile. The process repeats until convergence is achieved. The dynamic (vehicular) loads lead to an envelope of funicular profiles, which are then compared with a generic parabolic and a generic catenary profile of the same span and rise. Results like in-plane moments, horizontal thrust, vertical reactions, axial forces, deflections are compared.

KEYWORDS: Deck-Arch Bridge; Funicular; Graphic Statics; Parametric.

1 INTRODUCTION

There is immense scope for provision and improvement of road network connectivity, especially in the hilly regions of India and neighbouring states of Nepal, Bhutan, etc. (4). Amongst all types of bridge superstructure typologies, arch bridges have a significant scope in form-finding; funicular form-finding methods in arches have been explored in detail by stalwarts like Antonio Gaudi (for static loads) and bridge designers in particular like Robert Maillart (for moving loads). The idea behind a funicular shape is the transfer of loads through pure compression as inverted to a tied chain model with similar load arrangement hanging down due to gravity in pure tension (11)

While substantial research has already been done on funicular form finding in the past century, through the utilization of parametric tools and computer-generative form finding, a process for obtaining the ‘perfect arch’ can be developed in the case of both 2-hinged and 3-hinged Deck Arch Bridges.

In the current design practice, for a given span a rise is chosen by the designer

based on the aesthetic considerations. Circular arch/segmental arch profiles are chosen for masonry bridges of short to medium span and for steel bridges in some cases. The parabolic profile is mathematically proven to be better suited for uniformly distributed loads producing zero or minimum in-plane bending moments along the arch rib. Therefore, parabolic arch profiles are increasingly used for open-spandrel steel and concrete bridges in the past-half century.

1.1 Graphic statics

Graphic Statics is the field of structural mechanics that involves translation of algebraic problems of statics into graphical representations. The external forces are represented as force vectors and through basic vector algebra, they are resolved into resultant directions (12). Although graphical methods eliminate the use of error-prone arithmetic equations, they are on a decline now because the traditional methods of graphic statics involved the use of the classical hand draughting methods. This study reinvigorates the area of graphic statics through modern CAD modelling tools to solve and analyse arch problems.

In Graphic Statics, external forces are drawn to a predefined scale called the force scale. The actual line diagram of the structure (beam/truss/arch) is drawn to a suitable scale called the space scale. This diagram is called the structure diagram. Alongside, a polar diagram is converted with the same forces drawn in a line tail to end. With a suitably chosen polar point, radial lines are drawn originating from it towards the tails of each of the force vectors drawn within this polar diagram. Now these radial lines are borrowed from here to the structure diagram resulting in a funicular polygon. Since there is equilibrium of forces considered in the system, graphic statics is a self-checking process (15).

1.1.1 Eddy's Theorem

The Eddy's Theorem is a useful part of Graphic Statics that helps in quick analysis of the section forces through the use of the generated Funicular Polygon. It states that "the bending moment at any section of a structural element is proportional to the vertical intercept the pressure line and the axis of the structure." (14)

1.2 Funicular structures

A funicular structure is one which can achieve a stable equilibrium under the action of loads. The term funicular comes from the Latin word *funis* meaning rope. Just as a rope sags and assumes a curvilinear shape under its own weight, a funicular geometry is achieved under the action of a specific set of loads. To understand funicular structures a detailed understanding of a catenary is needed. (11). *(Figure 1)*

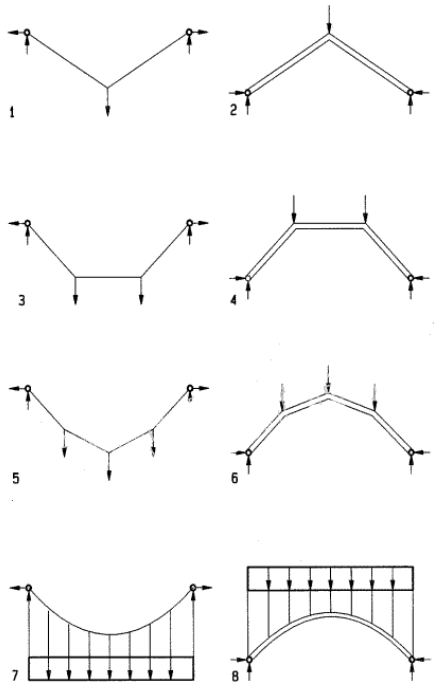

Figure 1. List of catenary string shapes with loads (left) with their respective funicular shapes (right). the funicular shapes are 'perfect' for the particular loads on the string. (11)

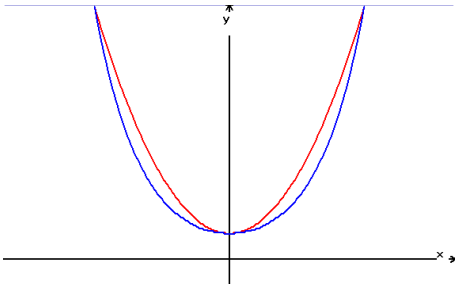

Figure 2. Difference in a parabolic (red) and a catenary profile (catenary).

1.2.1 Difference between parabolic and catenary arches

The Catenary curve is similar to the Parabola. The only difference is observed near the springing points, where owing to the greater slope of the sagging rope, the catenary weight distribution is much congested in the horizontal direction. As we move further towards the center, the cable becomes horizontal and the weight distribution stabilizes itself and becomes uniform. This results in greater deflections in the case of the catenary, as can be observed in the outward profile (blue) as compared with the parabolic profile *(Figure 2).*

2 TEST STUDY 1 - FORM FINDING FOR MOVING LOADS ON A 3-HINGED DECK ARCH

This section deals with form-finding of a three-hinged arch bridge girder of 25 m span with a set of defined moving loads. The permanent/static loads considered here were the self-weight of the bridge deck girder, the weight of the piers and the weight of the arch itself. Moving loads were applied to the scale of IRC 70R

(wheeled), but the entire chain was not applied. The bridge consisted of 5 bays of 5m each. The rise was kept at 9m. The deck would exert its self-weight and the loads on the moving loads on the piers and the two abutments. The abutments are of little interest here because they would either rest on the adjacent soil or as piers over the springing points. But the intermediate piers act as point loads on the arch. These loads combined with the self-weight of the arch would ultimately govern the funicular profile of the arch. *(Figure 3)*

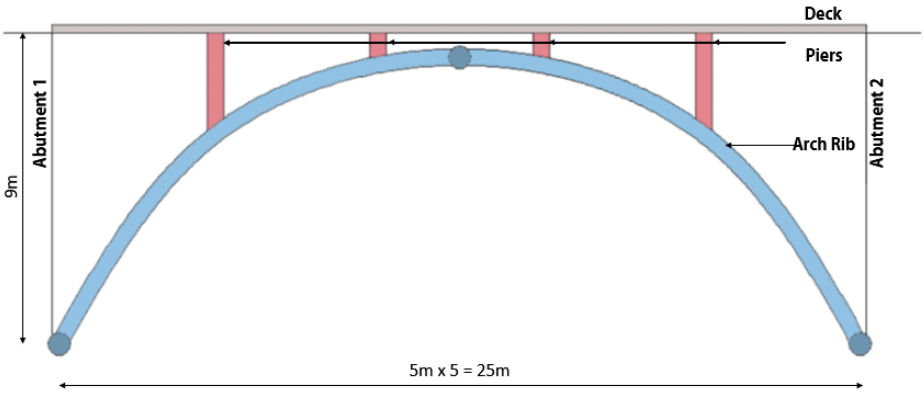

Figure 3. General arrangement of the bridge

2.1 The deck girder

For simplicity of the exercise, the entire bridge deck was idealised as an RCC single I section with a wide top flange as a single wheel lane *(Figure 4)*
Cross section area of the deck = 1.47 m^2
Depth = 2.025 m

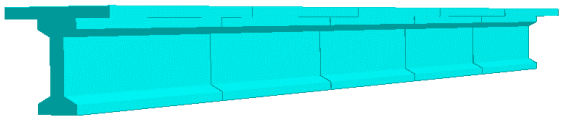

Figure 4. Rendered model of the girder

2.2 Moving loads

Figure 5 shows the definition of the moving loads adopted. There were four point loads of 80 KN, 120 KN, 120 KN and 180 KN spaced at 3.96 m, 1.52 m and 2.13 m. The Reactions RA1 and RA2 on abutments A1 and A2 were of no significance for the generation of the arch profile. However, the intermediate pier reactions R1, R2, R3 and R4 would directly affect the funicular shape of the arch as point loads.

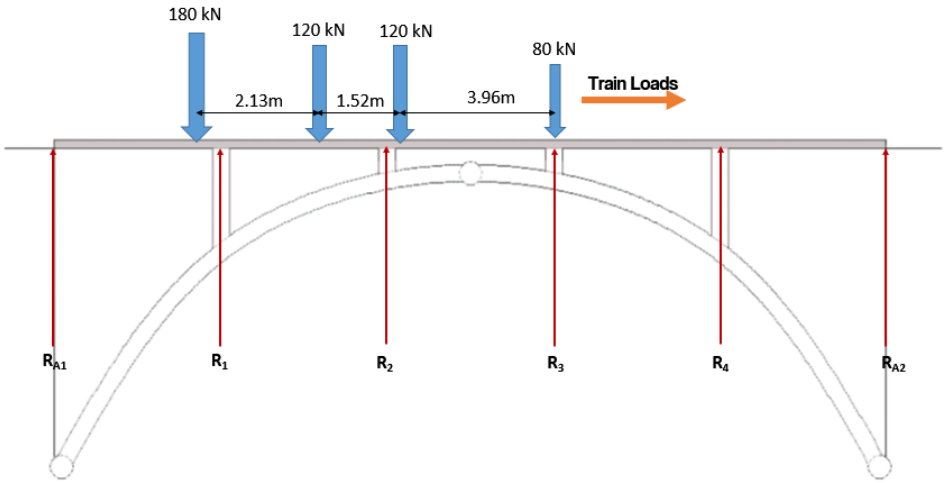

Figure 5. Moving loads' definition

2.3 Creation of load sets

Since there were four intermediate supports, four sets of values were obtained from the STAAD Analysis, each corresponding to that particular incremental load case which rendered the max value of vertical reaction at each of the four supports *(Figure 6)*.

The four sets of loads (R1-R4) obtained in the previous section were inverted and the self-weight of the RCC piers were added. Both of these loads together acted as point loads on the arch. With a fixed cross-section of 700 x 300 mm, the self-weight becomes a function of the length of the pier.

Weight per meter length of the pier = $0.7 \times 0.3 \times 25$ KN/m^3

= 5.25 KN/m

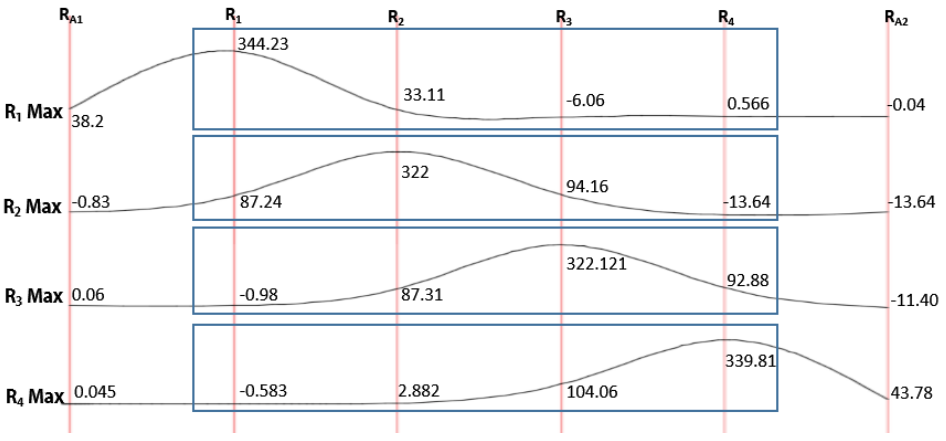

Figure 6. Load Sets with R1 to R4 Max each (specified on the left side)

2.4 Iterative process for pier length adjustment

Finding the length of piers was an iterative process – the initial arch geometry would govern the length (and therefore the self-weight) of the individual pier segment from the deck to the arch rib. This self-weight would significantly contribute as a point load on the arch governing the funicular shape of the arch in turn.

2.5 Self-weight of the arch

The cross-section of the RCC arch was assumed to be 700 x 1000 mm. The perfect preliminary shape for an arch considered here was a parabola with the given chosen rise of 9 m. The self-weight of an arch per unit length = $0.7 \times 1 \times 25$ KN/m^3 = 17.5 KN/m (3)

2.6 Use of graphic statics and computational programming in *Rhinoceros/Grasshopper*

The entire process of obtaining a funicular shape for the set of loads mentioned above was converted in the form of a parametric interface in the CAD software *Rhinoceros 3D* with the parametric plugin *Grasshopper*. The live interface would intuitively describe the bending moment behaviour across the arch profile. Furthermore, employing Eddy's Theorem, the exact numerical value of the Bending Moment across any section could be obtained. In the further sections, the algorithmic flowchart employed in the Grasshopper script shall be presented.

2.7 Input parameters

The input parameters listed governed the generation of the arch. They were all number slider components giving complete numerical control to the user. The various parameters are explained as follows:

1. *Force scale*: the representative drawing scale for the forces – 1 mm on the CAD interface would denote 10 KN of force. The direction of all forces were in the gravity direction, with the exception of the ones in the polar diagram where the forces are inverted/upward, drafted tail-to-head from bottom to top, as appearing left to right in along the span of the arch. (12)
2. *Space scale*: the graphic drawing scale – here 1 mm on the CAD interface represents 2 m in the actual drawing.
3. *No. of supports*: 6 - Piers plus two abutments. Only pier loads are considered to be of importance in the form-finding as the abutment loads don't fall on the arch rib but either on an approach pier or on the arch springing points
4. *Span*: 25 m
5. *Rise*: 9 m
6. R_1-R_4: Inverted Reaction Loads as obtained from the STAAD Analysis.
7. *Pier Linear Weight*: The Weight of the Pier per unit length as calculated above = 0.525 (*10 KN/m)

8. *Arch Self Weight*: The self-weight of the arch with a catenary distribution = 0.525 (*10 KN/m). Notice the closer/congested spacing of the vertical projections near the springing points and almost equal/flat distribution near the center.

2.8 Creating an envelope of funicular polygons

As shown in Figure 4.5, there were four sets of reactions corresponding to the maximum at each support, which needed to be inverted and fed along with the rest of the parameters of this program. In general, the number of possible sets of load values would be equal to the number of supports in any two dimensional deck-arch bridge problem. Therefore, four funicular polygons (Fig 4.23) were generated corresponding to the load sets illustrated in Figure 30. They were baked and assigned different colours in Rhinoceros.

2.9 Analysis of section moments using Eddy's theorem

In order to assess moments at various sections of the original parabola from the funicular polygon generated, Eddy's theorem was employed which goes as follows:

$$BM_x = [p \times f] \times [(y_1\ y_2) \times s], \quad \text{where}$$

p = revised polar distance
f = force scale
y_1 y_2= the length of the vertical intercept between the axis of the structure and pressure line at section x-x
s = space scale (12)

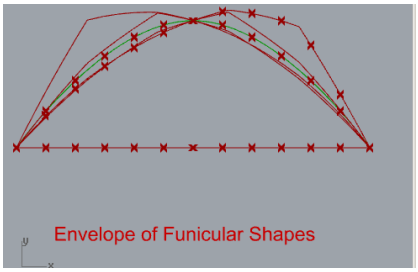

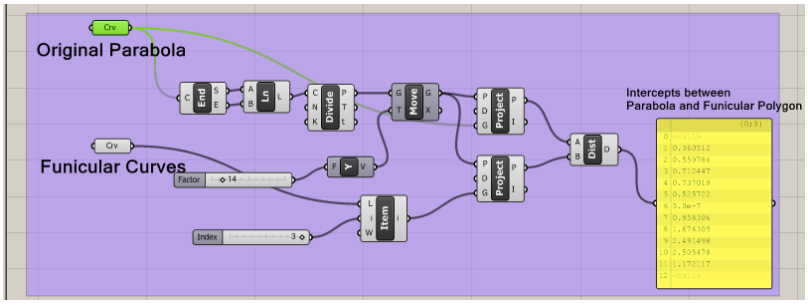

Figure 7. Finding intercept between parabola and the funicular curve

In order to determine the changing intercepts y_1 y_2 at various sections of the four funicular polygons, the code was written by creating a line segment between the two springing points and dividing into 12 segments *(Figure 7)*. The data was tabulated onto an excel sheet and bending moments at different sections were obtained *(Figure 8)*.

2.10 Observations

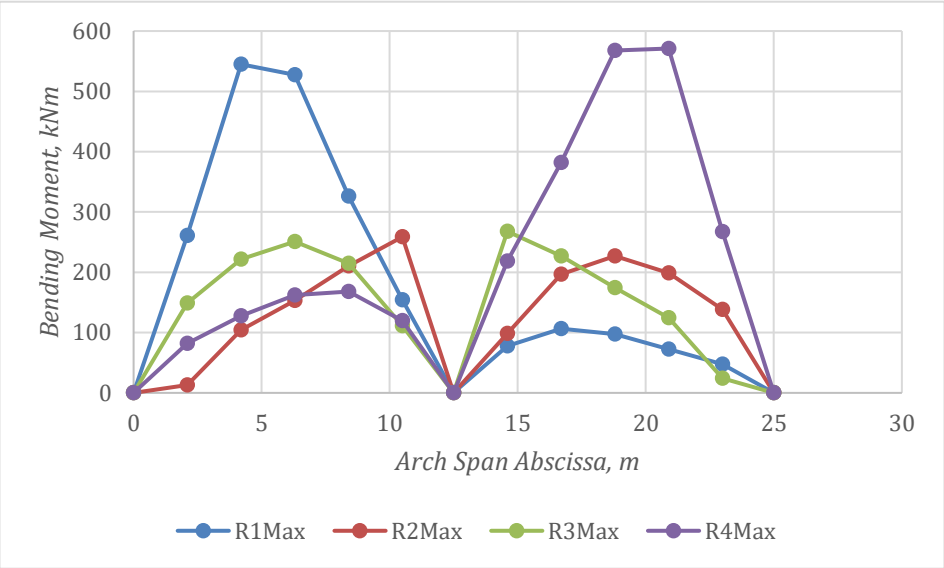

Figure 8. Bending moment at different sections along span of the 3-hinged arch

2.10.1 Effect of variable loads

- The variation of the funicular polygon depended on the ratio between the permanent static loads and the moving vehicle loads.
- Increasing the permanent loads to equal or more than the moving vehicle loads reduced the movement in the shape of the funicular polygons. (11)

2.10.2 The stiffening beam

One of the methods to reduce the deviations of the various funicular polygons achieved in the exercise could be through the introduction of a stiffening beam. In the bridge shown, the deck acts as a stiffening beam – 230 mm deep in this case – is designed to carry the moments due to the variable loads keeping the loads coming onto the arch more or less (11).

2.10.3 Using envelope of polygons to arrive at the optimal form

Once a set of profiles of all the funicular polygons were determined, the variation in the thickness of the arch at various sections was arrived at. By *Eddy's Theorem*

it was understood that greater deviation would amount to greater moment forces *(Figure 9)*.

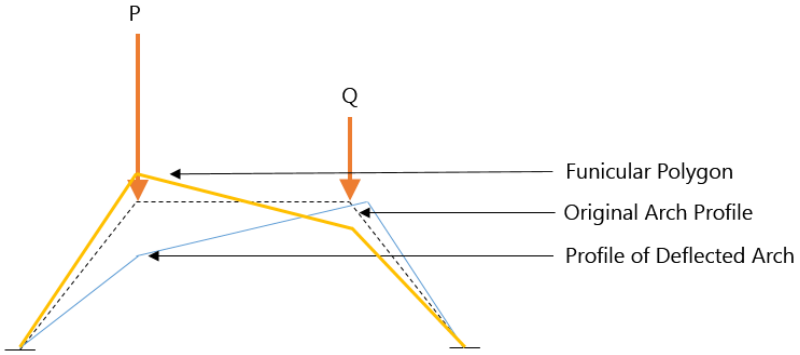

Figure 9. Movement of a funicular polygon under variable loads

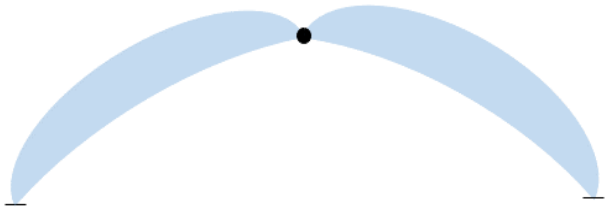

Figure 10. Optimal form of a 3-hinged form

Greater thickness was provided at probable sections with greater funicular movement so as to resist greater moments. These moments were a result of the moving loads, as the permanent loads would primarily decide the overall general shape of the arch. Moreover, keeping the arch section thick enough so that a funicular polygon would pass through the *kern* of the section would eliminate the possibility of any tension in the structure. (11) *(Figure 10)*

3 TEST STUDY 2 - FORM FINDING FOR MOVING LOADS ON A 2-HINGED DECK ARCH

Since the graphic statics approach of structural analysis is only applicable for determinate structures, a mathematical approach was chosen to carry out the form-finding for a 2-hinged arch which is an indeterminate structure. The funicular curve was generated from a beam model pinned at both supports, with the given set of loads – all considered as point loads – acting on a straight line, as on a taught horizontal string. The funicular shape was generated by adjusting the heights of each node so that the beam moment is nullified with the thrust moment and the vertical reaction moment. The following section shows the steps followed to arrive at a mathematical formula to obtain the funicular geometry.

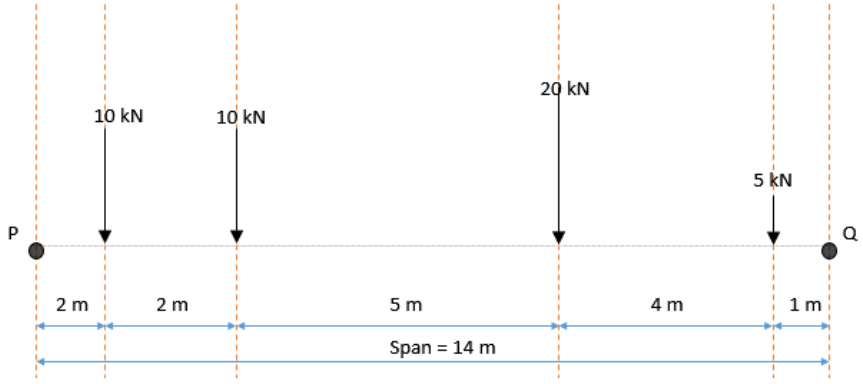

Figure 11. Arrangement of loads of a span of 14m

A span of 14 m with arbitrary loads acting in the gravity direction were assumed *(Figure 11)*. The lines of forces help in generating the funicular curve, hence the abscissae of the lines of forces were noted down. A matrix was created with m_i representing force lines abscissae (in meters) and n_i representing the forces (in KN) The height of the forces i.e. the ordinate was not taken into consideration. In fact, the suitable height is what was to be determined as per statics. The index *i* denotes the node number starting from *0*, which is the left most support. *(Figure 12)*

i	m_i	n_i
0	0	0
1	2	10
2	4	10
3	9	20
4	13	5
5	14	0

Figure 12. Matrix generated

3.1 Determination of unknowns

The information presented in the matrix generated was necessary and generated for determining the vertical support reactions.

We know that $\sum f_y = 0$, taking vertically up as positive,

$$\Rightarrow \quad R_P + R_Q - \sum_{i=1}^{i=5} n_i = 0$$

$$\Rightarrow \quad R_P + R_Q = 45 \qquad (1)$$

Also $\sum M_P = 0$, taking clockwise moment as positive,

$$\Rightarrow \quad R_Q = \frac{\left(\sum_{i=0}^{i=5} m_i n_i\right)}{m_5}$$

$$\Rightarrow R_Q = \frac{305}{14} = 21.78 \text{ KN} \quad (2)$$

Put eq. (2) in eq. (1),

$$\Rightarrow \quad R_P = 23.22 \text{ KN}$$

3.2 Rise-thrust relation

As per statics, the equation to find the horizontal thrust *H* in a two-hinged arch is given by:

$$H = \frac{\int M_0 y \, ds}{\int y^2 ds} \quad (3)$$

Where,

M_0 = beam moment at a section,

y = ordinate of the arch at that section

ds = infinitesimal arch element where s is the length of the center-line of the arch

However, the approach to find the thrust in this case was different. It was assumed that the greatest sag under a similar string/rope model would occur under the greatest load or at the centre of gravity of loads.

3.2.1 When greatest sag is assumed under the centre of gravity of loads

For a discretized load model like in Figure 11, the abscissae of the centre of gravity on the span would be

$$CG_x = \frac{\{(0\times0)+(10\times2)+(10\times4)+(20\times9)+(5\times13)+(0\times14)\}}{0+10+10+20+5+0}$$

$$= 6.78\, m \text{ (From left support)}$$

$\Rightarrow$ Nearest node at $i = 3$, where $m_i = 9$, $n_i = 20$ *(Figure 13)*

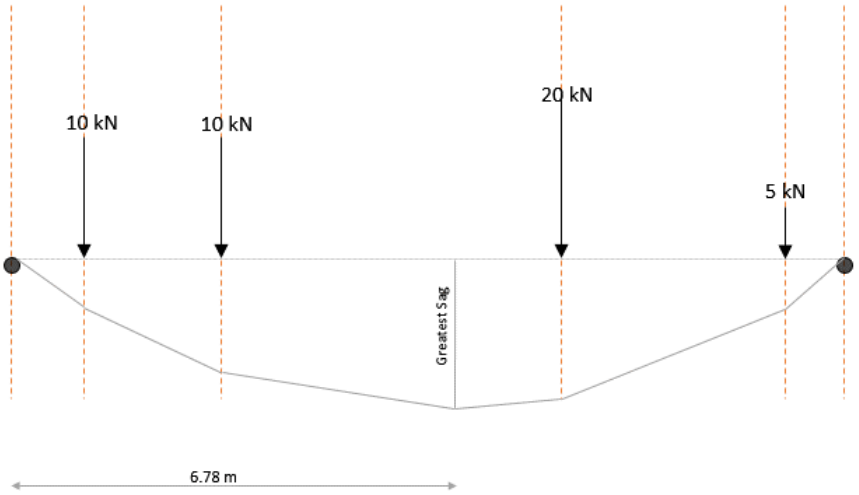

Figure 13. When the greatest sag is under the CG of loads

3.2.2 When greatest sag is assumed under the greatest load

After determining R_P and R_Q, and fixing a rise for the arch at a particular location, the only unknown left to be determined was the horizontal thrust. Through statics, equating the moment at the crown of the arch to zero, the horizontal thrust was found, as explained in the next section.

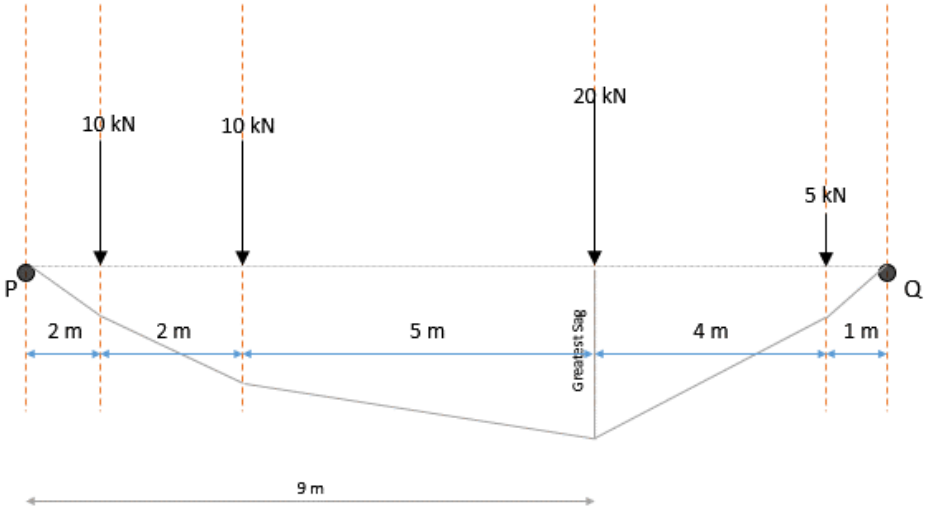

Figure 14. Greatest load is at i = 3, where $m_i = 9$, $n_i = 20$

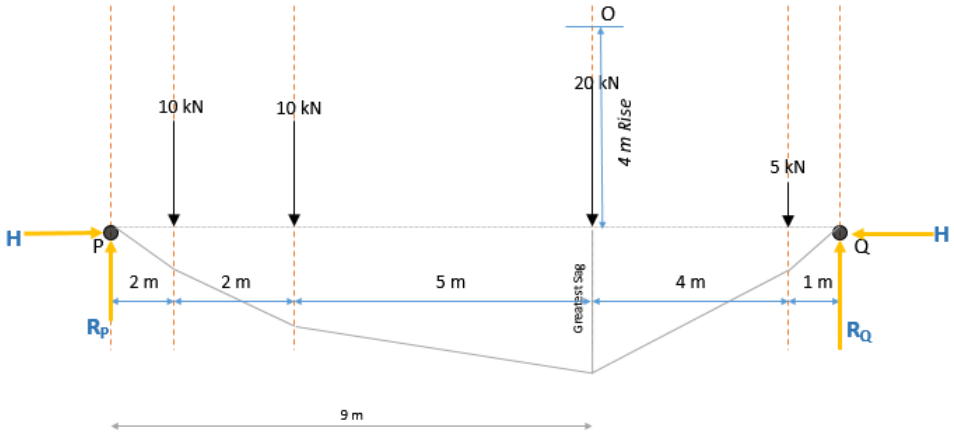

Figure 15. Point O is the crown at the desired Rise (4m)

Equating the moment on the left side of crown node O to zero

$$\sum M_o = 0$$

$$\{10 \times 5\} + \{10 \times (5+2)\} - \{R_P \times (5+2+2)\} + \{H \times 4\} = 0$$

$$H = \frac{\{R_P \times (5+2+2)\} - \{\{10 \times 5\} + \{10 \times (5+2)\}}{4}$$

$$= \frac{\{R_P \times 9\} - \{\{10 \times 5\} + \{10 \times (5+2)\}}{4}$$

$$= \frac{208.98 - 50 - 70}{4}$$

$$= 22.245\ kN$$

The above sequence can be formulated as:

$$H = \frac{\{(R_P \times abscisccae\ of\ crown\ node) - (Beam\ moment\ towards\ left\ of\ crown\ node)\}}{Rise}$$

Using matrix terminology,

$$H = \frac{\left[(R_P \times m_i) - \left\{\sum_{j=0}^{j=i-1} (m_i - m_j) \times n_j\right\}\right]}{Rise}$$

Where *i* is the index of the crown node O

3.3 Funicular heights for all nodes

Once all the force unknowns – the vertical reactions and the horizontal thrust – were determined, further employment of equations of static equilibrium gave the funicular heights of each node. In other words, the height of each node was adjusted such that the moments at each these nodes would come to be zero. (12). *(Figure 16).*

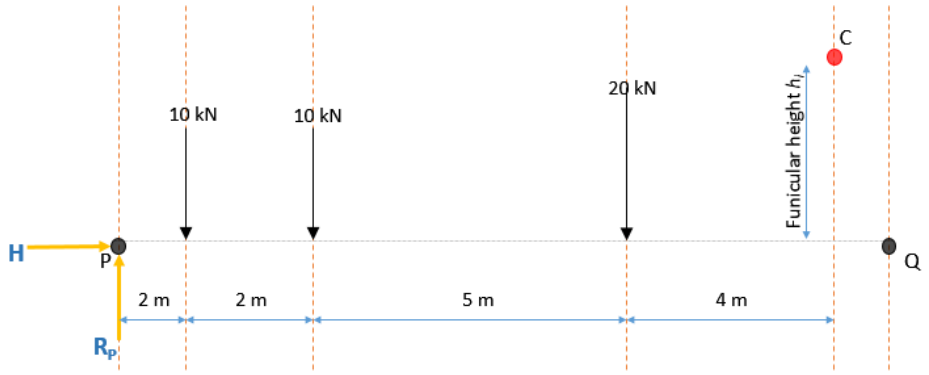

Figure 16. Adjusting the funicular heights

A point *C* was adjusted at a height such the beam moments to the left i.e. moments due to 20 KN and both the 10 KN loads and those due to vertical reaction R_p and the thrust *H* cancelled each other out, giving the net moment at C as zero.

$$\sum M_{c_{left}} = 0$$

$$(20 \times 4) + (10 \times 9) + (10 \times 11) - (R_P \times 13) + (H \times h_i) = 0$$

$$h_i = \frac{(R_P \times 13) - \{(20 \times 4) + (10 \times 9) + (10 \times 11)\}}{H}$$

$$= \frac{(23.22 \times 13) - (280)}{22.245} = 0.98$$

The above calculation can be generalised for any force line at index *i* as:

$$h_i = \frac{(R_P \times abscissae\ of\ index\ force\ line) - (Beam\ moment\ left\ of\ index\ force\ line)}{H}$$

$$h_i = \frac{\left[(R_P \times m_i) - \left\{\sum_{j=0}^{j=i-1} (m_i - m_j) \times n_j\right\}\right]}{H}$$

This equation was used to generate the funicular heights at every force line. For the height of point *C* whose calculation has been demonstrated i.e. at *i=4*, the element h_4 can be seen as 0.98. Similarly, other funicular heights were generated and tabulated *(Figure 17).* As a check, at three critical points – the two springing points and the crown – the heights confirmed the credibility of this method. At the springing points, i.e. at *i=0* and at *i=5*, the funicular heights were 0, confirming their level at the datum of the polygon. Also, h_i at the crown (*i=3*) was 4 viz. the rise of the arch *(Figure 18).*

i	m_i	n_i	h_i
0	0	0	0
1	2	10	2.088
2	4	10	3.27
3	9	20	4
4	13	5	0.98
5	14	0	0

Figure 17. Matrix with a column of funicular heights h_i added

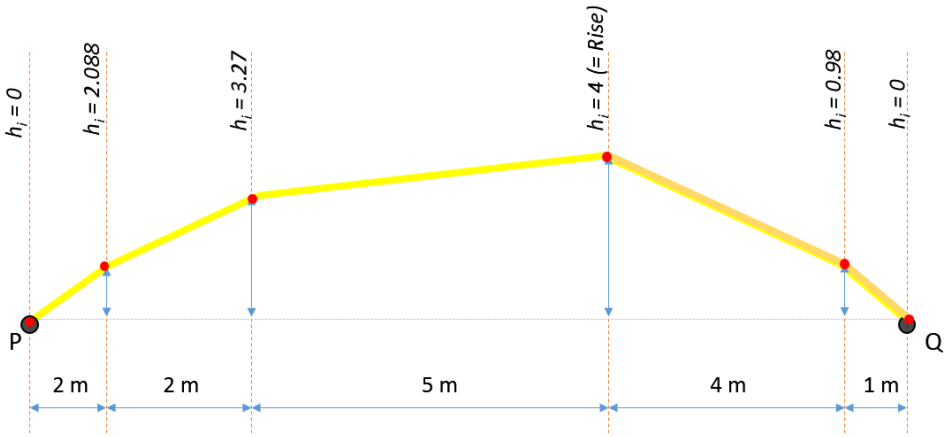

Figure 18. Funicular polygon formed (yellow) by joining the points at different funicular heights (red)

3.4 Modelling the script in *Rhinoceros/Grasshopper*

The mathematical process could be easily translated into an interactive program in any software or any spreadsheet like *MS Excel*. In this exercise, owing to the ease in programming of a visual programming editor (VPE) like *Grasshopper* with in-built mathematical functions with real-time parametric control, it was considered suitable to model the entire process by scripting it in *Grasshopper*. In the later section of this study, for the generation of arch profiles in the design of a full-fledged 265 m arch, the same program is employed to generate a series of arches.

3.5 Verifying Results through structural analysis

In order to confirm the results obtained through this *Rhinoceros/Grasshopper* mathematical model, a structural analysis of the *.dxf* model exported from *Rhinoceros* was carried out in structural analysis software *Bentley STAAD.Pro*. The results obtained from *STAAD* analysis matched with those of *Rhino* to a satisfying degree. The minute sections forces arose due to the stiffness of the members *(Figure 19).*

(kN)	From Rhino+GH	From STAAD
R_P	23.214	23.214
R_Q	21.785	21.786
H	22.232	22.248

Figure 19. Comparison of results of reactions

4 FORM FINDING AND ANALYSIS OF 265 METER SPAN DECK-ARCH BRIDGE

Having obtained a process for a two-hinged arch in the previous section with a given set of loads, it was deemed possible to utilise the same in a full-fledged deck-arch bridge superstructure design problem. The problem of a hypothetical bridge with a span of 265 m was chosen. A general arrangement drawing was drafted which gave details of the width of lanes, the deck sections, the spans, placing of piers, etc. Accordingly, starting from the modelling of the deck to that of the piers, the loads were analysed and a set of matrices were created to generate the funicular shapes with a pre-decided rise. Thereafter structural analysis was done on the different arches with the above-mentioned to deduce, verify and compare the force results. Comparison of forces were also drawn with a parabolic arch of the same span and rise. Based on the force results, suitable sections of arch rib in CFT (*Concrete Filled Tubes*) were developed and chosen. The load matrices were modified, with the added arch self-weights. Funicular shapes were again generated and observed. The loads considered for this process are supplemented in Annexure-A.

4.1 Formulating the design problem

A hypothetical bridge design problem was chosen to implement the form-finding process discussed so far over a full-fledged deck-arch roadway bridge at Anji Khad in Jammu, India where the proposed span of 265 m was chosen *(Figure 20).*

4.2 Design basis

- Height of Bridge (between F.L. and B.L.): *189 m*
- Type of Bridge: CFT Deck Arch Open Spandrel Type
- Design Arch Span: *265 m* (Symmetrical Arch assumed)
- No. of Lane: 2+2+footpath on both sides
- Spans (metres): *{(1 x 30) + (3 x 25) + (1 x 15) + (1 x 12.5)} x 2 ways*
- Type of Deck: Composite Slab with Steel Girders
- Type of Arch Rib: CFT with a series of Rectangular Hollow Sections.
- Rise: *60 m*
- Loading: 2 lanes of Class A or 1 lane of Class 70R loading each way of traffic.
- Codes consulted: *IS 800, IRC 6, IRC 112, IRC 22, IRC 24, BS 5400 (parts 3* and *5)*

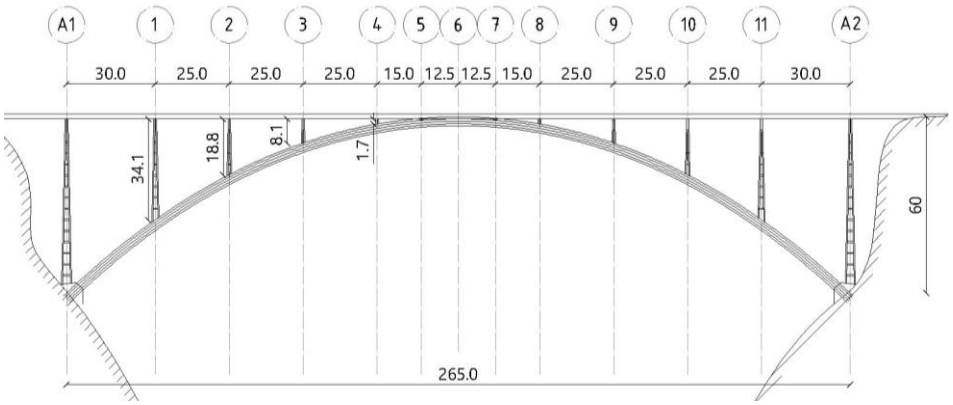

Figure 20. Bridge elevation (dimensions in meters)

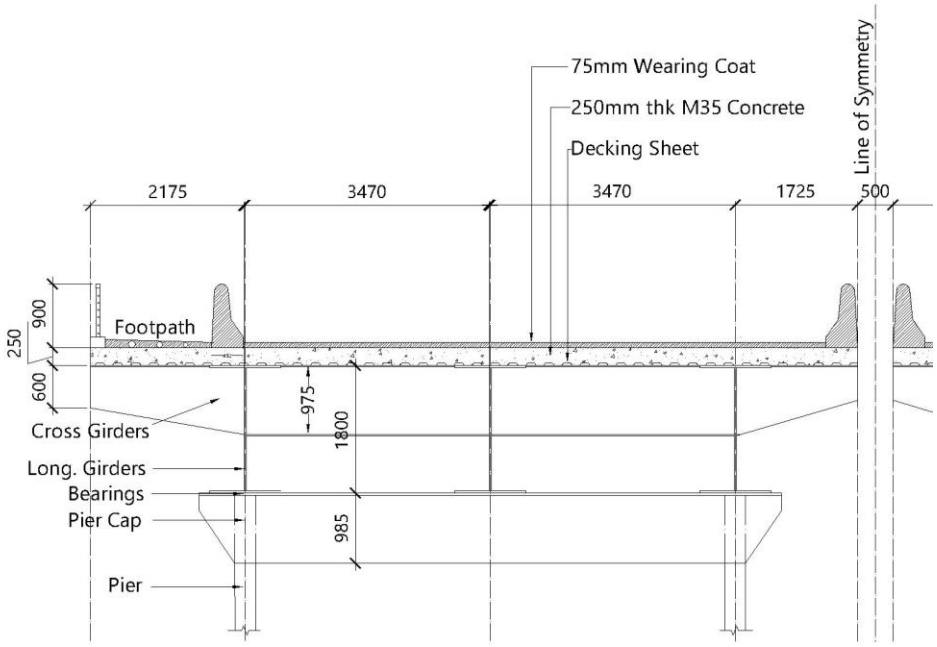

Figure 21. Cross-section of a one-way 30m span at the support (dimensions in mm)

4.3 Composite deck

The deck was proposed as a composite girder slab system with plate girders running simply supported bearing-to-bearing longitudinally *(Figure 21).* They were interspersed with transverse girders at *0.5 m* to *1 m* with profiled top flanges designed to transfer shear to the longitudinal plate girders. The top flanges of both the girders flush to accommodate the profiled decking sheet upon which rests the concrete slab with minimum shrinkage reinforcement. The composite action is facilitated by the shear connectors. On the top is a *75 mm* wearing coat.

4.4 Grillage modelling

The analysis of the deck was performed by grillage analogy method. This method involves dividing the deck into a two-dimensional grid with the gridlines running in the two orthogonal directions – one along the span, parallel to the longitudinal members, and the other perpendicular to span. The girders have an effective flange width for the necessary slab actions as per the codes. They are assigned their material properties in the analysis software or given the equivalent moment of inertia in both the directions along with the torsional moment of inertia *(Figure 22)*.

Three grillage models were created for the analysis of the deck – first with only self-weight of all the structural members and the super imposed dead load, second with incremental loading of two lanes of Class A chain and third with incremental loading of one lane of Class 70R chain. A total of 2000 load cases in both Class 70R and Class A cases each were generated.

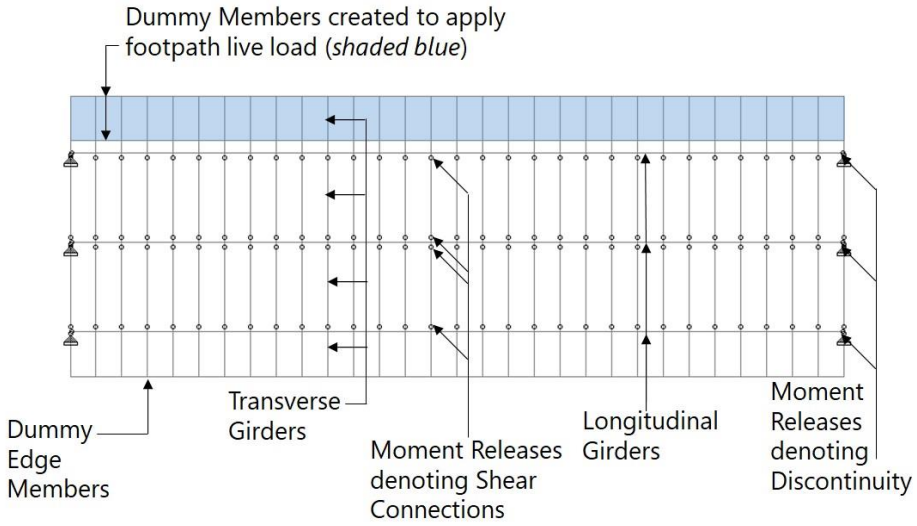

*Figure 22. Ele*ments of a sample grillage model of one span explained in plan

4.5 Post analysis

Once all the three deck grillages were analysed, the reactions obtained from each of the bearings were noted down and tabulated. The reactions at the abutment bearings (terminal nodes) were ignored. The other bearings were important as reactions on those would be transferred to the arch rib.

4.6 Critical load cases

For the live load grillage models, an envelope of maximum reactions on each of the bearings were noted along with their corresponding incremental load case was

considered. These load cases were marked as *Critical Load Cases*. The number of such load cases marked the number of matrices that would be obtained for the funicular curve generation.

4.7 Converting bearing loads into pier loads or reaction sets

Since the study deals with in-plane forces and deals with the generated funicular arch in two dimensions, the three bearing loads from each of girders were added and were condensed into the respective 11 pier loads. In other words, Reactions were shrunk into what formed *46* Reaction Sets. By a '*Reaction Set'*, what implies is a set of all those forces that might be inverted and said to be acting over the Piers. These forces were required to:

- Design the Piers
- Act as loads for the funicular arch generation

4.8 Pier self-weight

Once the bearing reactions were obtained, pier sizes were determined through codal design provisions (1), (2) for axial compression plus biaxial bending. The bending moments were assumed to be arising due to the eccentricities of an envelope of the forces on the bearings. Groups of four angle sections with stiffening plates were chosen for the pier. The center line length of these piers were measured from the bearings to the top edge of a preliminary catenary arch generated. The self-weight of these piers was added to the bearing loads obtained. The three central piers were deemed too short (less than a metre in length) for any significant load hence they are marked with red crosses at the top. *(Figure 23)*

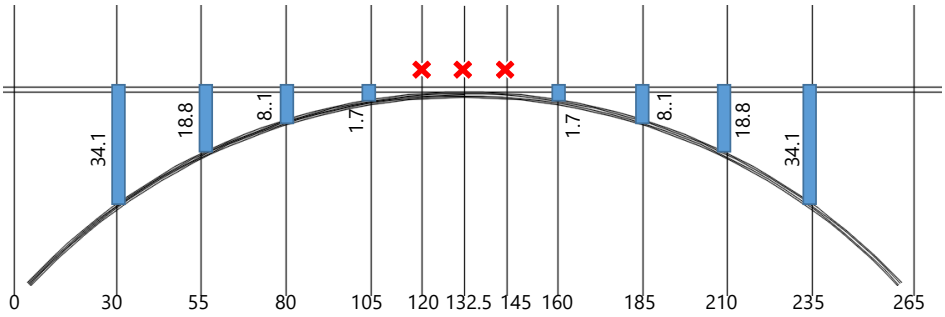

Figure 23. Piers considered with their length (in blue) along with their abscissae

4.9 Generating load matrices

Once the reactions due to dead loads, super imposed dead loads, live loads and impact loading were obtained from the grillage analysis, the pier loads were added and *46* load matrices were obtained. These load matrices helped in the generation of the funicular arches as explained in the previous

section. The index *i* denotes the node number starting from the leftmost node of the arch *0*. The first column m_i denotes the abscissae of the position of the loads whereas the column n_i denotes the magnitude of loads acting in the downward direction. As shown in Table 6.10, there were *46* matrices generated (only some of the n_i values are shown) pertaining to the total of *46* reaction sets.

4.10 Generation of funicular shapes in *Rhinoceros/Grasshopper*

The program created in *Grasshopper* to draft funicular shapes in *Rhinoceros* has been explained in the previous chapters. The *46* load matrices mentioned above were fed into the same code *(Figure 24)* where the list m_i comprised of the abscissae/X-Coordinates of the application of the loads whereas the list n_i comprised of all the possible sets of loads to applied to generate the funicular arches.

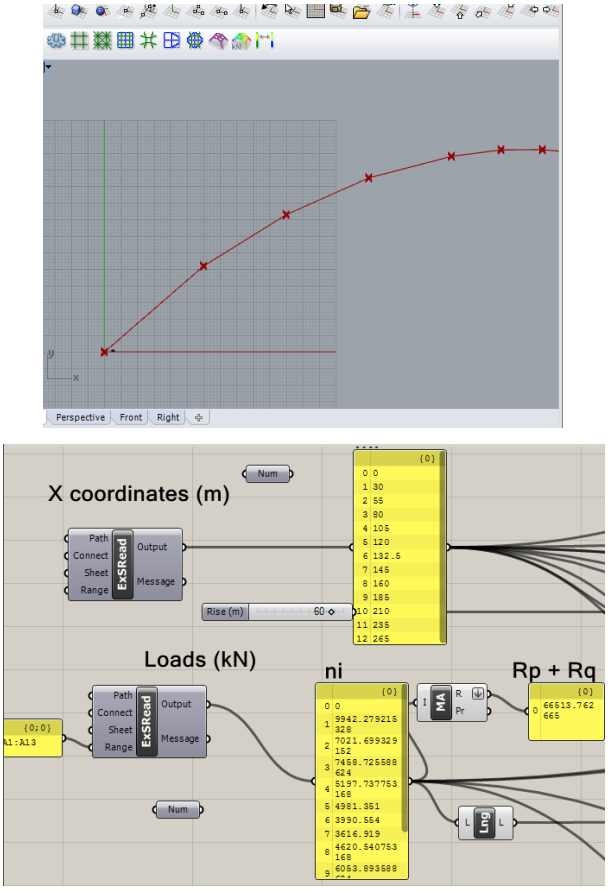

Figure 24. Funicular shape generated in Rhinoceros

As a result, keeping the list m_i fixed, a call was made to each and every one of the *46* sets created into the list n_i. Therefore, a total of *46* funicular arches were generated using this script. A visual observation was carried out by super imposing a parabolic arch and a catenary arch over the *46* arches.

4.11 Structural analysis

A structural analysis of some of the chosen curves out of 48 curves (46+Catenary+Parabola) was carried out in *STAAD.Pro*. The 46 load reaction sets were chosen as nodal loads to be applied on the 11 intermediate nodes of each curve.

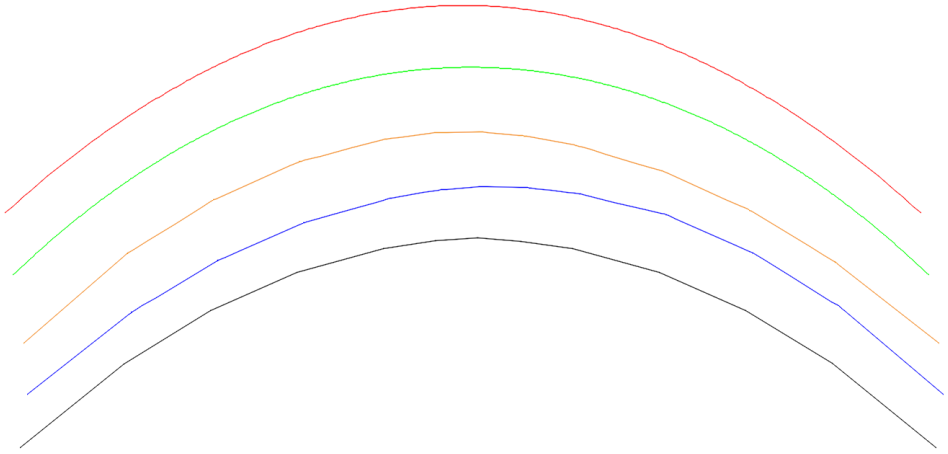

Figure 25. Curves: red – parabola; green – catenary; orange – leftmost leaning funicular; blue – rightmost leaning funicular; black – normalized curve

4.12 Arriving at a normalized curve

One of the curves upon which structural analysis was performed was a *normalized curve* generated from the envelope of 46 funicular arches generated. In order to arrive at the node of a normalized curve, each of the junctions of the envelope were zoomed in for observation, and all the 46 nodal points of that node were identified. Then a centroid of the 46 nodal points was located. This procedure was repeated for all 11 nodes. All the centroidal points were all joined to form a polygon *(Figure 26)*. Also, out of these curves, 5 prominent curves, namely (i) Parabola, (ii) Catenary, (iii) Leftmost leaning Catenary, (iv) Rightmost leaning Catenary and (v) Normalized Curve, were extracted for further investigation *(Figure 25)*

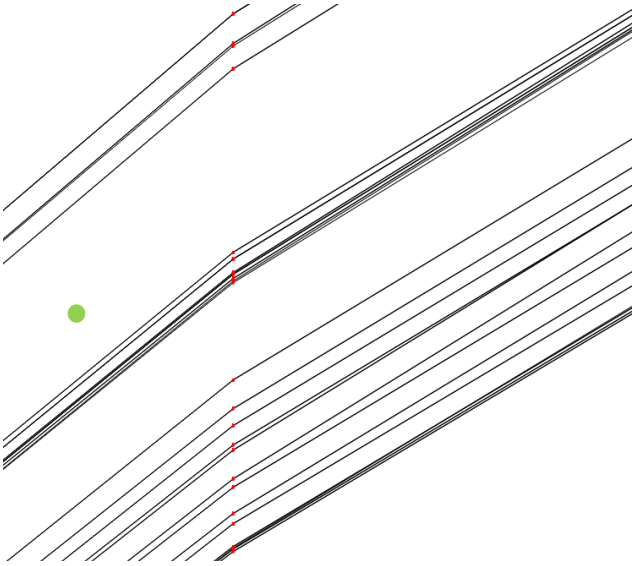

Figure 26. Detail at a node of the envelope of curves – The green point is the centroid of all the red points shown and shall itself act as a node of the normalized curve.

4.13 Arriving at CFT sections

Data such as in-plane moment $M_{x,}$ in-plane shear V_y, axial force along the arch rib, vertical support reactions and the horizontal thrust was tabulated. Rectangular Steel Sections were chosen for the rib. Here the entire arch rib was assumed to act as a composite column with an axial compression plus uniaxial bending. *BS 5400 part 3* and *5* were referred for the design guidelines.

4.14 Modification of load matrices

After the finalization of the CFT Section of the Arch Rib, the Load Matrices were modified to add the linear self-weight of the CFT arch. The m_i which denotes the abscissae for the application of the loads, was varied with an increment of *0.5* meters. This implied that at every increment from left to right, the value of n_i was fed as half the linear self-weight of the arch rib i.e. *83.208 KN/m*. At positions of applications of pier and deck loads, the loads from the previous generated 46 matrices were added to the linear self-weight.

4.15 Generation of final funicular arches

Once again, the 46 load matrices were fed into the program script developed in Grasshopper and the 46 funicular arches were baked superimposed onto one another to obtain a final envelope of arches.

5 RESULTS AND CONCLUSIONS

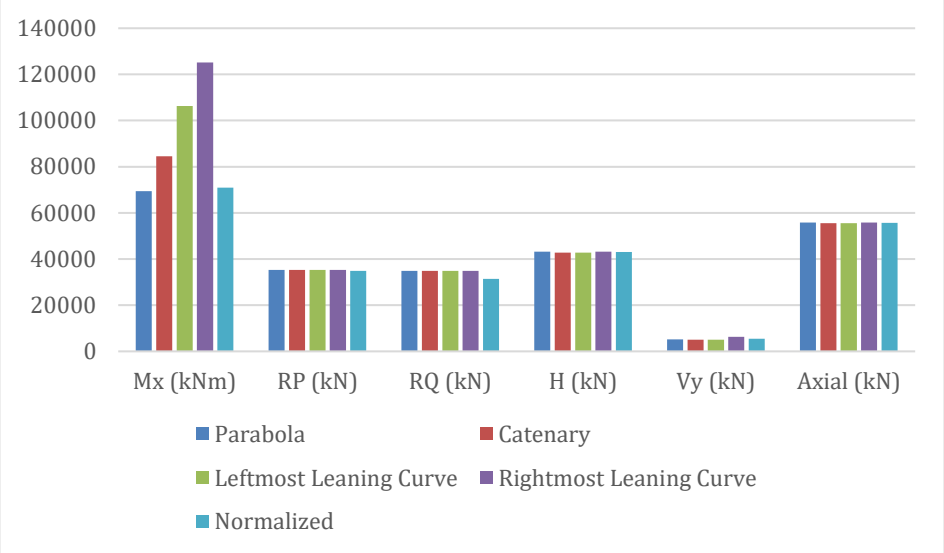

Figure 27. Forces before application of arch self-weight (from STAAD analysis)

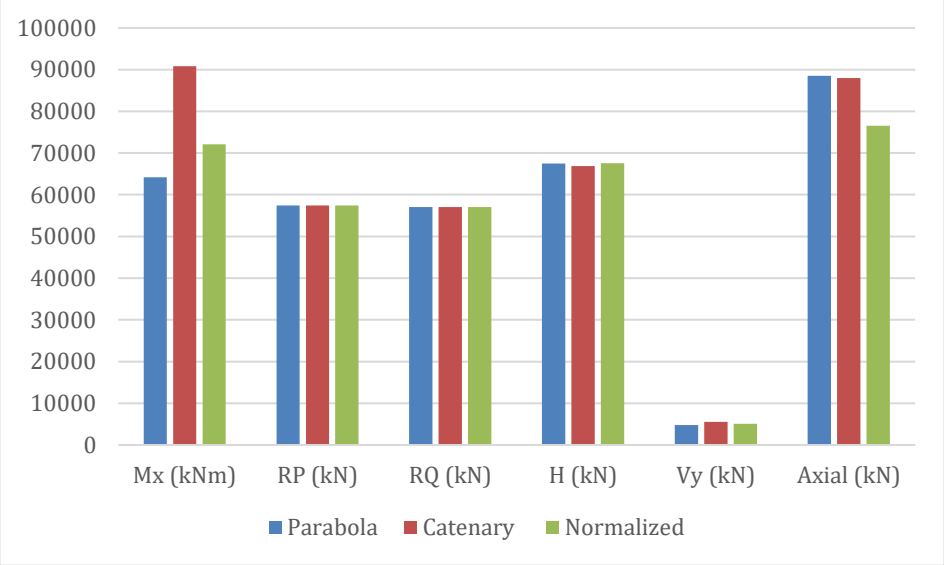

Figure 28. Forces after application of arch self-weight (from STAAD analysis)

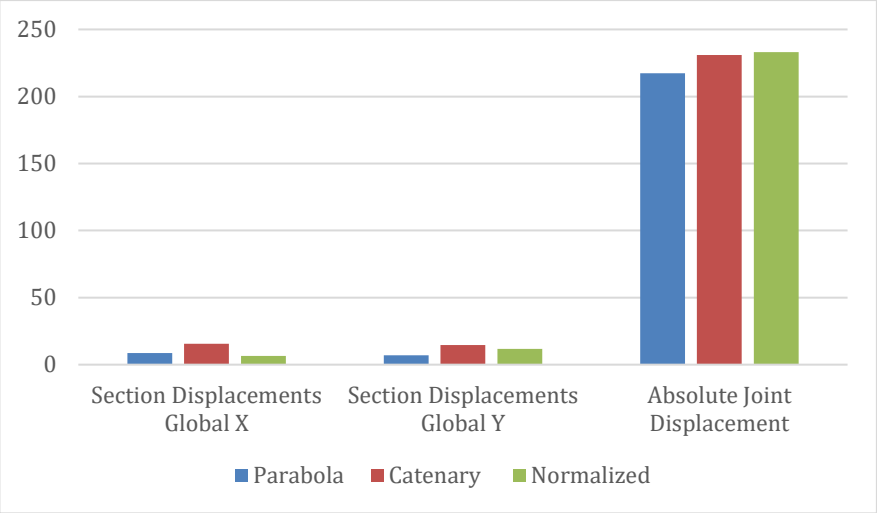

Figure 29. Rib deflections in mm (from STAAD analysis)

5.1 Observations and inferences

- For the final design problem, 5 arches were analysed for 46 load cases before the application of the self-weight and 3 arches after the consideration of self-weight.
- It was observed that the Parabola and the Normalized curves generated almost similar in-plane bending moments which were considerably lower than the other three curves. The rest of the forces were comparatively similar in magnitude *(Figure 27).*
- After the CFT Arch Rib self-weight was considered the Parabola curve generated the lowest bending moments. However, in turn it resulted in the highest axial forces *(Figure 28).*
- The Normalized curve generated higher bending moments but lower axial forces (lowest in all) than the parabolic curve.
- The Catenary curve and the Rightmost leaning and Leftmost leaning curves gave unfavourable results in all cases. However, the Catenary curves generated slightly lower horizontal thrusts in all cases.
- The parabolic curve underwent the least displacements *(Figure 29).*

Based on the above observations the following preferences could be made on the selection of arches.

Force to minimise	In-Plane moments	Horizontal Thrust	Axial Forces	Displacements
Type of Curve	*Parabola*	*Catenary*	*Normalized*	*Parabola*

5.2 Future scope

- The structural system studied were predominantly two-dimensional. However, using advanced form-generating methods like *Thrust Network Analysis* could be employed to generate form-active structures in three dimensions. (13)
- Consideration of lateral forces – Wind and Earthquake forces – on the arches could be studied and an analysis and design process could be developed.
- Feasibility and behaviour of CFT arch ribs under specifically wind loads – either by CFD techniques or more comprehensively wind tunnel modelling and analysis – over conventional steel or RCC ribs can be studied.
- Optimization of material by variation of amount of concrete in the CFT Sections along the arch profile as per the change in section forces can be studied
- A different flow of generation of funicular arches could be devised based on the construction sequence.

6 REFERENCES

1. BS 5400:2000, Part 3, Part 5
2. IRC-24; IRC-6:2014, Part-2, IRC-112
3. IS 800:2007, IS 875
4. Narayan, Laxmi (March 2006). "Technical Paper on Anji Khad and Chenab Bridges" (pdf). Advances in Bridge Engineering: 101–114
5. www.steelconstruction.info/Tied-arch_bridges
6. Victor, David Johnson. Essentials of Bridge Engineering.
7. Namin, Aria Aghajani. "Structural Evaluation of Tied-Arch and Truss Bridges subjected to Wind and Traffic Loading". Thesis, Masters in Science – Civil Engineering, Eastern Mediterranean University, June 2012.
8. Joysar, Mahesh P. "Analysis and Limit State Design of Concrete Filled Steel Tube Through-Arch Bridge." Thesis, Department of Civil Engineering, Institute of Technology, Nirma University, Ahmedabad, Gujarat, India, May 2014.
9. Nguyen, S H; Bradford, M A., "Design Strength of Slender Concrete-filled Rectangular Steel Tubes".Paper, The School of Civil Engineering, The University of New South Wales, Kensington, Australia.
10. Pelly, R J. "A Critical Analysis of the Bayonne Bridge, New Jersey". Paper, Proceedings of Bridge Engineering 2 Conference 2009, University of Bath, UK
11. Muttoni, Aurelio. "Art of Structures: Introduction to the Functioning of Structures in Architecture". Book, Oxford EPFL Press 2011.
12. Rao, D. S. Prakash."Graphical Methods in Structural Analysis". Textbook, Hyderabad Universities Press (India) Ltd. 1997.
13. Lachauer, Lorenz; Jungjohann Hauke; Kotnik Toni. "Interactive Parametric Tools for Structural Design". Paper, IABSE ETH Zurich
14. Thadani, B. N. "Graphic Statics". Book, Bombay Weinall Book Corp. 198
15. Benson, Cyril S. "Graphic Statics". Book, London B.T. Batsford Ltd. 196
16. Fairman, Seibert; Cutshell, Chester S. "Graphic Statics". Book, London,Boston etc McGraw Hill Pub. 193
17. Johnson, R. P; Buckby, R. J. "Composite structures of steel and concrete. Vol. 2: Bridges with a commentary on BS: 5400-(Part.5)". Book, London Crosby Lockwood & Son Ltd. 1979.

ANNEXURE A - LOADS CONSIDERED

- *Dead Loads*
  Load of Steel Plate Girders
  - For *30 m* and *25 m* spans,
    Left Girder and Centre and Right Girders = *11.59 KN/m* Linear Load
  - For *15 m* and *12.5 m* spans
    Small Left Girder and Small Centre and Right Girders = *6.913 KN/m* Linear Load
  - For Transverse Girders, ISMB 600 = *1.21 KN/m (*Self Weight)

  Load of Concrete Slabs
  - *250 mm* thickness, density of RCC = *25 KN/m^3*, Floor Load = *6.25 KN/m^2*
- *Superimposed Dead Loads*
  - Load of Wearing Coat, *75 mm thick* Macadam, density = *22 KN/m^3*, Floor Load = *1.65 KN/m^2*
  - Load of Crash Barrier + Railings

Area of Crash Barrier	=	*0.257*	*m^2*
C.B. as Point load	=	*6.425*	*KN*
Railing Point load	=	*0.15*	*KN*

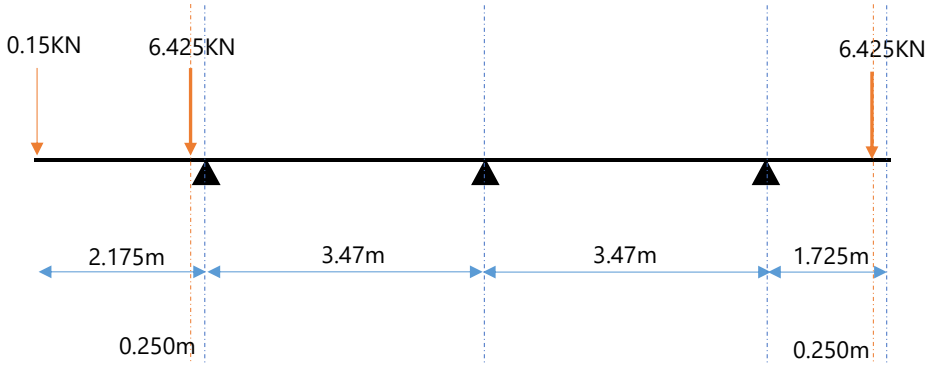

Schematic section of deck showing crash barrier loads and railing loads

- *Footpath Live Load*
  Although it is a termed as a live load, the Footpath Live Load was considered as a Superimposed Dead Load and applied as a distributed floor load over the area designated for footpaths.
  As per *Cl. 206.3* of *IRC 6 2014*
  "*For effective spans of over 7.5 m but not exceeding 30 m, the intensity of load shall be determined according to the equation*:

$$\boldsymbol{P} = P^1 - \frac{40L - 300}{9}$$

Where $P^1 = 400\ kg/m^2$

Footpath Live Loads for different spans

Span	=	30	25	15	12.5	m
P	=	300	322.2222	366.6667	377.7778	kg/m^2
	=	3	3.23	3.67	3.78	KN/m^2

- *Primary Live Load*
  For a carriageway width of *8.2 m* distributed over 2 two lanes in one way, the codal provisions of *IRC 6 2014* allow either 2 lanes of Class A Loading or 1 Lane of Class 70R Loading.
- *Impact Factor*
  As per Cl. 208.2 of IRC 6 2014
  "In the members of any bridge designed either for Class A this impact percentage shall be determined from the following equations which are applicable for spans between 3 m and 45 m."
  Impact factor fraction for steel bridges (span L) = 9/(13.5+L)
  For Class 70R loading (wheeled) for steel bridges, as per Cl. 208.3 of IRC 6 2014 25% impact factor was to be taken for spans up to 23 m. For spans larger than 23 m, Fig 5 of IRC 6 2014 was referred.

(Transverse Girders)

Table 1. Impact factors for different spans

Span (m)	30	25	15	12.5	3.45	2.175	1.725
Class A Steel	1.207	1.234	1.316	1.347	1.531	1.545	1.545
Class 70R Steel	1.147	1.147	1.22	1.25	1.25	1.25	1.25

- *Secondary Live Load*
  As per *Cl. 211.2* of *IRC 6 2014*
  "In the case of a single lane or a two lane bridge: twenty percent of the first train load plus ten percent of the load of the succeeding trains. Where the entire first train is not on the full span, the braking force shall be taken as equal to twenty percent of the loads actually on the span or continuous unit of spans."
  Also, as per *Cl. 211.3* of *IRC 6 2014*
  "*The force due to braking effect shall be assumed to act along a line parallel to the roadway and 1 .2 m above it. While transferring the force to the bearings, the change in the vertical reaction at the bearings should be taken into account."*

Table 2. Longitudinal Forces transferred to the bearings

Class A							
Span		=	30	25	15	12.5	m
Total Load		=	554	554	500	418	kN
Force $_{Left}$		=	4.432	5.3184	8	8.0256	kN
Force $_{Right}$		=	-4.432	-5.3184	-8	-8.0256	kN
Class 70R							
Span		=	30	25	15	12.5	m
Total Load		=	1000	1000	1000	830	kN
Force $_{Left}$		=	8	9.6	16	15.936	kN
Force $_{Right}$		=	-8	-9.6	-16	-15.936	kN